ORIGINAL PAPER

A Review on SAR Image and its Despeckling

Prabhishek Singh[1] · Manoj Diwakar[2] · Achyut Shankar[1] · Raj Shree[3] · Manoj Kumar[4]

Abstract

The method of speckle reduction is widely used in synthetic aperture radar (SAR) imagery over the last three decades. The SAR images are inherently speckled in nature. Speckle noise is a granular pattern distribution, usually modeled as a multiplicative noise that affects the SAR images, as well as all coherent images. Other SAR related problems are also discussed in this paper. Therefore, despeckling approaches are needed to improve the quality of SAR images. However, there is a trade-off between speckle reduction and the preservation of fine details in the despeckled SAR image. The reduction of the speckle noise without losing the fine details of the SAR image is a difficult task. However, many despeckling methods have been discussed to reduce the speckle noise from the SAR images. Each method has their own norms, advantages and disadvantages. This article contains a review of some major work in the field of SAR image despeckling. Often, scientists and scholars have faced the struggle to understand the pattern distribution of the speckle noise in SAR images. Hence, a brief details about radar, SAR imaging, speckle noise in SAR images and the prevalent approaches of SAR image despeckling are reviewed here. The advantages and disadvantages of SAR image despeckling approaches are also analysed and discussed.

1 Introduction

SAR images are the greater perseverance images of a broader landscape of the earth's surface that is captured by the special form of radar called SAR. SAR images are inherently speckled in nature due to constant constructive and destructive collision of the transmitted high-frequency radar waves with target areas. The nature of speckle-noise is multiplicative. The effect of speckle-noise on the SAR image is comparatively more adverse than the other types of noise. In 1980, Lee JS proposed the first solution for the reduction of both additive and multiplicative speckle noise using neighborhood intensity values in the kernel [1]. Here the pixels are processed separately. It efficiently eliminates the speckle noise but the fine details are distorted in the image like edges. The solution of the filter [1] was later systematically established in [2] and revised in [3] incorporated with the sigma filter.

1.1 Background

Radar (Radio Detection and Ranging [4, 5] or Radio Direction **a**nd Ranging [6, 7] is an aperture that employs radio signals to detect and compute the speed, angle or scale of objects. It is employed in the detection aircraft, ships, guided missiles, and forecasting and constraints of the atmosphere. Radar that featured with emitters and the primary work of the emitters to emits the high-frequency electromagnetic signals towards targets. The emitting and receiving antenna is used for emitting the radar signals and receiving the dispersed information. The receiving antenna and processor determines the characteristics of the objects.

✉ Achyut Shankar
  ashankar2711@gmail.com

  Prabhishek Singh
  prabhisheksingh88@gmail.com

  Manoj Diwakar
  manoj.diwakar@gmail.com

  Raj Shree
  rajshree.bbau2009@gmail.com

  Manoj Kumar
  wss.manojkumar@gmail.com

1   Department of CSE, Amity School of Engineering and Technology, Amity University Uttar Pradesh, Noida 201303, India

2   Department of CSE, Graphic Era (Deemed To Be University) Dehradun, Dehradun, Uttarakhand 248002, India

3   PI (CSTUP), Department of Information Technology, Babasaheb Bhimrao Ambedkar University, Lucknow 226025, India
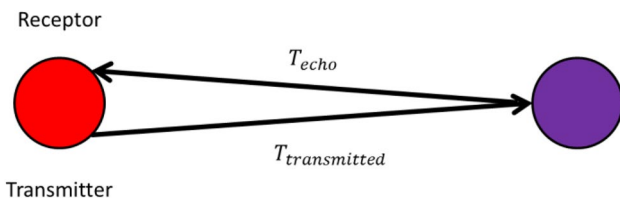
4   Department of CSE, UPES, Dehradun 248002, India

Receptor

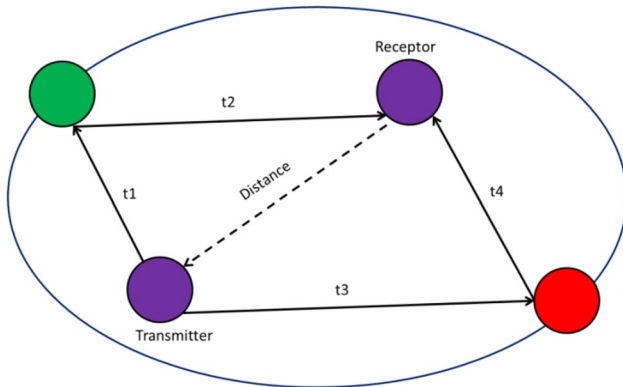**Fig. 1** The basic mechanism of an active radar system

Fig. 2 Basic mechanism of a passive radar system

Radar is categorized into two types:

- Active radar and
- Passive radar.

In active radar, an antenna emits high-frequency radio waves on the objects of the earth's surface and echoes back the backscattered information of the object. This type of radar is called mono-static. In Fig. 1, the variable T denotes

the time delay that is equal to the total time taken by the signal to be transmitted to the object and reflected back i.e. ttransmitted + techo. Here the location of the transmitter and receptor is the same.

In a passive radar system, the location of the transmitter and receptor is different. A passive radar system depends on the signal spread from a dissimilar location. This type of radar system is called bi-static. In the Fig. 2, t1 + t2 = t3 + t4. This condition is true for every object that is positioned on the ellipse of Fig. 2. For both of the objects in Fig. 2, from the receptor point of view, the time delay amid the real signal and the obtained backscattered signal is exactly the same. The function of the passive radar system is highly relies on the number of transmitters and receptors and their geometry.

Radar is categorized into two main groups on the basis of antenna size:

- Real Aperture Radar (RAR)
- Synthetic Aperture Radar (SAR)

1.1.1 RAR

RAR is the non-coherent radars that are governed by the physical length of the antenna. It is an active radar that transmits high-frequency radar waves from the antenna to the particular piece of terrain that one wants to obtain the image. This transmitted radar waves of the narrow-angle beam towards scale direction at right angles to the flight direction called the azimuth direction and getting the dispersion from the expected targets that will be changed to a radar image from the obtained signals, as shown in Fig. 3. The image perseverance is defined by the length of the antenna. It is impractical to design a big antenna as in to obtain a high-resolution image because in

Fig. 3 (**a**) A radar pulse is transmitted from the antenna to the ground (**b**) The radar pulse is scattered by the ground targets back to the antenna [9]

(a)

(b)
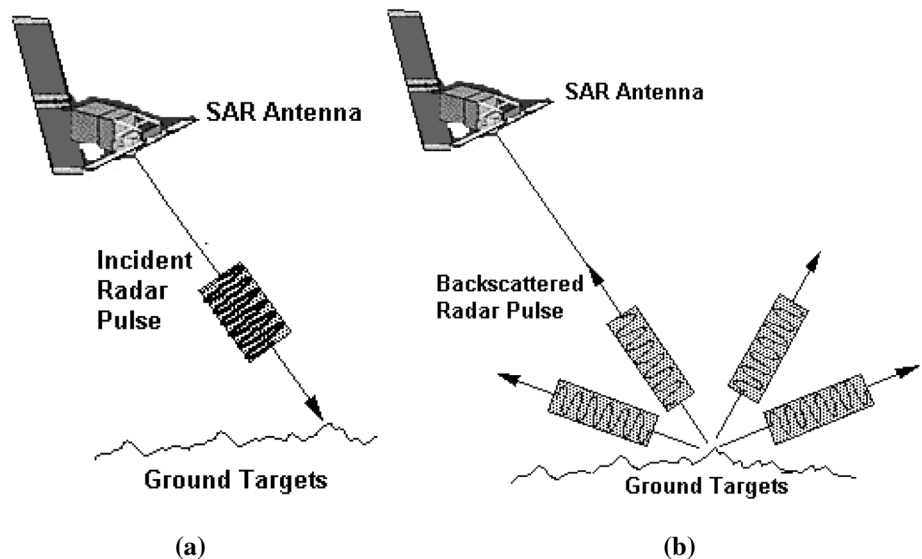
that case, an antenna has to be at least many times of the length of wavelength in order to minimize the bandwidth of transmitted signal [8]. If in case, such antenna is made then it is very problematic to mount such antenna, which requires 1 km diameter length of the antenna to get 25 m resolution with L band (= 25 cm) and 100 km distance from a target, a RAR hence has a practical constraint for refining the azimuth resolution.

1.1.2 SAR

In SAR imaging, the primary work of an antenna emits the microwave pulses towards the earth's surface. This high-frequency microwave energy dispersed to the aircraft is computed as shown in Fig. 3 [9]. The SAR using the fundamental of radar to create an image to make uses of the latency of the dispersed signals. SAR is the coherent radar that is added to the satellites and spacecraft that captures the high-resolution images of the huge surface area of the earth. SAR overshadows photographic and else optical imaging strengthen as it has the advanced capability of taking images in varying atmospheric circumstances, day and night due to various wavelengths of camera sensors. SAR performs over the sensors of the wavelength from 1 cm to 1 m, whereas camera sensors make use of wavelengths closer to visible light or 1 micron. Due to this difference, SAR has the capability to see through clouds and storms, whereas optical sensors are unable to do so. On comparing with RAR, SAR enlarges the size of the antenna or aperture synthetically to raise the azimuth resolution. In SAR, the data deal with the obtained signals and phases from changing targets with a compact antenna is a complicated process.

When radar waves stricks the earth's surface, the proportion of energy dispersed to the sensor as shown in Fig. 3 depends on many factors [9, 10]:

- Physical factors like dielectric non-variable of the surface components which also rely strongly on the humidity factors.
- Geometric factors like the roughness of the surface, inclined, substance improvement in regards to the radar signals.
- Classification of the land surface (soil, agricultural or artificial objects).
- Microwave frequency, polarisation and incident angle.

As the cloud-penetrating quality of microwaves, SAR is capable of acquiring "cloud-free" images in all climates [10]. This is particularly useful in tropical areas that are often under cloud cover during the whole year.

The greater quality as an active remote sensing aperture, it has ability to work in night-time operation [9, 11].

1.2 Different Types of SAR

SAR imaging is categorized on the basis of the nature of the application. The traditional SAR image processing is based on the strip mapping mode [12, 13]. This mode is used when the large terrain is to be captured. Here the terrain data is acquired without staring at any particular location. Heavy computation is required. In this SAR mode, a large unit of backscattered energy is bounced back and received by the antenna, which takes more computation time for handling this much data. Another type of SAR is flying SAR system i.e. spotlight mode SAR that stares at an exact scene typically on the ground [12, 13]. It captures a small terrain area than strip mapping mode hence requires less computation cost. It captures multiple SAR images of the same spot of the terrain to get more accurate data. Here multiple SAR images are captured within a time interval of seconds. Since the area of the captured region is not large, so the amount of reflected energy received by the antenna is not much. Due to this, the computational time is less. The spotlight mode is used in the applications where lower mapping, low processing time and low cost is the need. This mapping is heavily used by fighter aircraft to keep informed of the navigation system by tracing the recognized landmarks [13].

1.3 Applications of SAR

SAR has become one of the valued remote sensing tools for both soldierly and non-combatant users. Various soldierly SAR applications are intelligence gathering, battlefield survey, and weapons supervision. The non-combatant applications like agricultural and land-use monitoring, topographic planning, geology and mining, oil spill observation, sea ice observation, oceanography and planetary or celestial examinations [11]. SAR has wide practical applications on ocean as well as on land like artificial illegal or coincidental spills are visible in SAR images in the oceans, ships detection and tracking in the oceans, observation of natural leakage from oil deposits in the oceans, providing hints for the oil industries, ocean wave forecasting and marine climatology, regional ice monitoring. This is very crucial and helpful for navigation in ice-infested waters [11].

Other applications are monitoring lands of forestry and agriculture, in the impact of a flood, the greater quality of SAR to infiltrate clouds is extremely useful. With the help of the SAR data, it is very easy to optimize response initiatives and to assess damages, detecting small region

movements caused by earthquakes, landslides or glacier advancement [11].

2 SAR Image Creation

SAR is also like a camera that captures images. Both SAR and optical cameras have different penetrating capabilities. This penetrating capability depends upon the capturing phenomenon. In order to create an image, the optical camera depends on the light while SAR relies on radar signals which it transmits. This important difference of SAR allows capturing the images in pure darkness and also permits to see through clouds, rain, fog, and snow. Defining the SAR image requires a heap of data and terrific calculating power [14].

Mainly, the basic working principle of radar i.e. RAR is to calculate the time taken by the radio wave traveling from an antenna to object and back to the origin. Radar determines the traveling distance from an antenna to object and back to the origin to make use of time interval but this type of radar can only detect an object and calculate speed. To define the SAR image, an importantly huge heap of data and terrific calculating power is needed. It requires an exceptionally elongated antenna. But in SAR, it uses a smart way of synthetically creating a high length antenna by moving a small antenna to cover a wide distance. After getting all the information, it saved and starts processing it [14].

As the airplane flies and moves forward, the SAR antenna transmits the high-frequency radio waves also called radar waves towards the ground. In the middle of pulses, the antenna collects backscattered high-frequency radio waves that have considered objects on the ground. These disperse waves carry information that includes the total distance traveled by the pulses to make the round trip, from and to the aircraft. It also carries information about the movement of the SAR whether it is moving in the direction of or against the object on the earth's surface. The dispersed waves are recorded and if the pulses

are recorded to be very close to each other, then the plane with the SAR antenna is changing the position towards the ground and if the pulses are recorded to be far from each other the spacecraft is moving away from the ground [14].

From the greater amount of dispersed pulse information collected, there are some pulses that show a distinct shape, this distinct shape denotes that those pulses are considered from the same location. During this process the information related to distance is known from the accurate location the plane was when it was sent and pulses that fit the shape were found, It is quite simple information to plot the object's point on the image that is creating it. [14]. The point on the image is plotted, but the point illumination is still unknown. SAR calculates the illumination by the intensity of the signal it obtains. An object like tree absorbs radar energy and therefore appears gray. A metal back toward the SAR antenna reflects a lot of object-oriented energy, so it shows bright [14]. In SAR image processing, one thousand calculations are required to be done for each pixel. and such an image is shown below of Washington, D.C., which is made up of several million pixels in Fig. 4.

2.1 Roughness and Brightness of SAR Image

The brightness and darkness in the SAR images are due to the structure surface of the target object on the ground. The roughness of the surface decides the brightness of the SAR images. When the antenna transmits the high-frequency radar waves and they hit the ground, only a chunk of the signals back to the origin. The antenna has the capability of both transmitting and receiving the radar signals.

When the adequate chunk of the radar signals back to the origin then those parts are shows bright in the SAR image. When a very small chunk of the radar signals is reflected back to the origin then those areas are projected dark in the SAR images. There are certain factors over which the returning radar signals depend upon like electrical properties, roughness, the geometrical positioning of the surface and the polarization direction of the returning radar wave. Figure 5 shows the bright and dark areas in the SAR image.

Fig. 4 SAR image of Washington, D.C. took on a snowy night in 1994 [127]
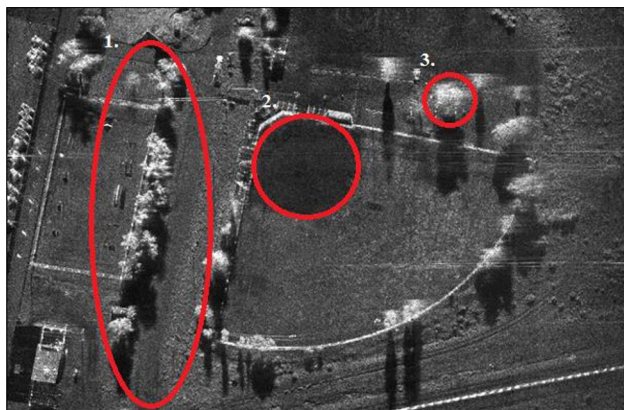
Fig. 5 Dark and Bright areas of the SAR images

Figure 6 shows the surface inclination of the target ground over which the radar signals strick. The smooth and rough surfaces are shown in the above figure. When radar signal hits the smooth surface of the terrain as shown in Fig. 6a the incidence angle of the radar signal is almost equal to the reflections angle of the reflected radar signal. This means that there is either no radar return or very less energy reflects back to the antenna. In this situation, the projection is shown dark in the SAR image. This type of case is mainly seen in the calm water body like a river that has a specular reflection [15].

When radar signal hits the rougher surface which has a random and irregular surface orientation, then the radar energy is backscattered in many directions as shown in Fig. 6b. In this case, a small portion of the radar energy is backscattered and received by the antenna which produces a bright signature in the SAR image. This type of case is mainly seen in SAR images of rocky mountains and trees.

The orientation of the local surface of the target region relative to radar wave travel path is responsible for the variation of brightness in the SAR images. Other various surface orientations responsible for variation in brightness are

shown in Fig. 7. When radar signal hit the surfaces that are perpendicular to the travel path of the signal then this scenario generates the strongest return as they are directly facing the sensor shown in Fig. 7a.

The slopes that face away from the SAR sensor produce the weak returns of the target information. Similarly, the slopes of the hills are steeper than the depression angle then they are not illuminated by the radar signals and are completely shadowed and in this case, least or no information of the returned back to the antenna which also appears darker in the SAR image. As the depression angle becomes smaller causing more gentle back slopes to become shadowed.

The visual appearance of the buildings in the populated area is bright and clear in the SAR image because of the corner reflector shape as shown in Fig. 7b and c. In Fig. 7b, corner reflector is shown that produces the strongest return of the radar signals. It can be noticed that the radar signals when hit the surface it completely reflects back to the SAR sensor regardless of the depression angle. The objects with metal surfaces like bridges and towers of power line appear brighter in the SAR images because the value of the dielectric constant is high [16]. The dry natural materials like rammed earth and earth sheltering have low dielectric constants, but the occurrence of humidity in the soil, snow, or vegetation raises this value and their radar reflectivity too. SAR image processing assesses humidity content of surface materials.

3 Problem in SAR Image

There are a number of reasons of disturbance in the performance of the SAR system and degradation in the quality of SAR image. Some of the reasons are nonlinearities of the SAR subsystem that damage the ability of the system resolution. Noise is one frequently seen problem in SAR images whose major source is image acquisition [17]. Other sources

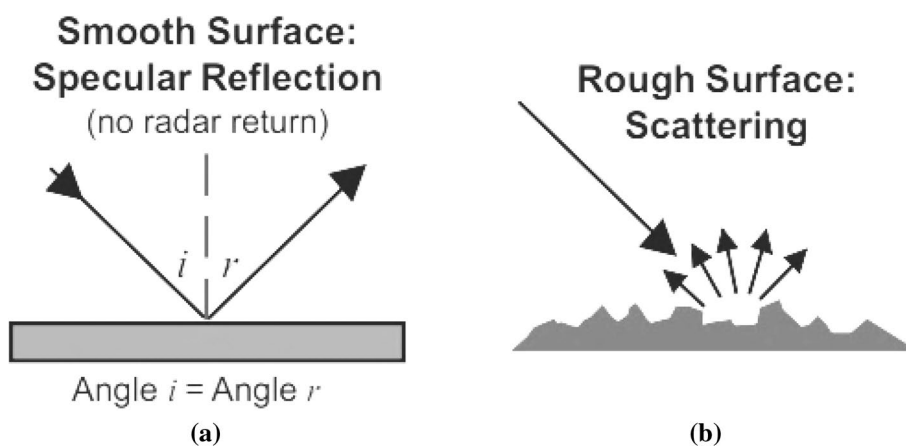**Fig. 6** Surface orientation (**a**) Smooth surface (**b**) Rough surface

(a)

(b)

Fig. 7 Surface orientation affecting the brightness of the SAR images
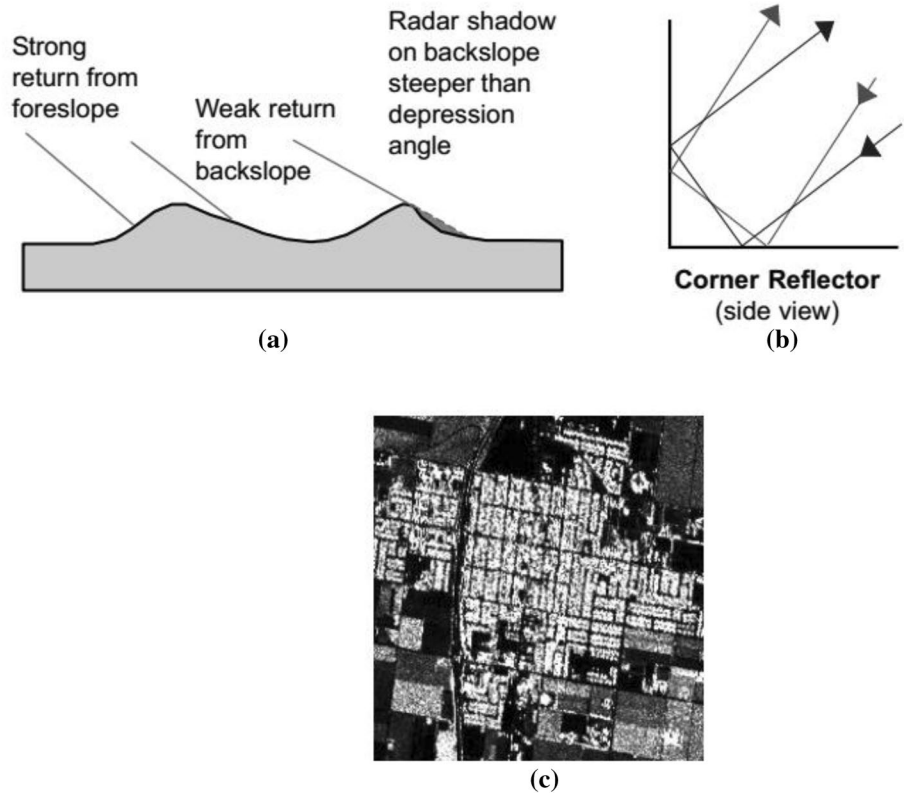

(a)

(b)

(c)

Table 1 Real problems in SAR images [13, 15, 16, 111]

Real effects on SAR images	Major sources
Geometric distortion	Change in position: movement variation and changes in platform attitude (high and low frequencies) cause distortion due to the platform of spaceborne or airborne
	Rotation of earth, topographic effect and curvature cause distortion due to earth
	Deviation in sensor mechanism and viewing geometry: panoramic effect causes distortion due to the sensor
	Refraction and turbulence cause distortion due to the atmosphere
	Time-variations or drift and clock synchronicity cause distortion due to measuring instruments
System nonlinear effects	Amplitude error and phase error degrades the system impulse response function (IRF)
	Thermal noise damages the dynamic range of the system
	Quantization error, bit error noise and system nonlinearities damage the azimuth resolution and dynamic range of IRF
Range migration	Linear drift because of elliptical orbit and earth rotation
	The appearance of hyperbola shaped reflection as target move towards the synthetic aperture
	Curvature depends on range compressed response due to which SAR handles the two-dimensional space-variant problem
	High velocities of airplanes and satellite-borne SAR apertures
Speckle noise effects	SAR images are formed by the constant collision of the emitted high-frequency radar waves with target areas. This constant collision causes random constructive and destructive nosiness that outcome in salt and pepper noise all over the image. This noise scatters all around the image and suffers from the speckle noise effects and reduce the property of the SAR image. It is a granular pattern noise that inherently found in the SAR image
	The existence of multiple fundamental scatter with an arbitrary distribution within a perseverance cell

of noise introduction are the position of sensor and velocity errors that result in geometric distortion in the SAR image. Major occurring problems in the SAR image are discussed in Table 1.

3.1 Noise in SAR Image: Speckle Noise

The granular shape that generally exists in the SAR image either during image obtaining or due to arbitrary constructive or destructive interference is known as speckle noise. It becomes visible like 'salt and pepper' noise due to its granular shape. The constant collision of high-frequency radar waves with a complex bunches of scatterers is possibly the minimum implicit and restrictive aspect of SAR processing model design and application.

Non-coherent sensors typically use radiation restricted physical apertures for the focusing of incident electromagnetic diffraction, followed by detectors that are sensitive to the total intensity of incident diffraction on them [18].
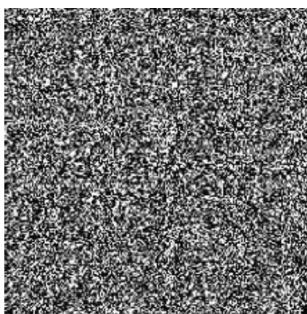

Fig. 8 Classical speckle pattern [18]

The traditional speckle pattern is shown in Fig. 8. Basically, speckle is not a noise but a scattering phenomenon [19, 20].

Speckle noise is produced as a multiplicative noise [21]. The speckled noise intensity serves as the randomly distributed multiplicative noise of the SAR image $F_L(i, j)$, Here the SAR image is considered as a mean of L looks that may be equated as,

$$F_L(i,j) = I(i,j) \times R_L(i,j) \tag{1}$$

In which $R_L(i, j)$ depicts the random variable of the speckle noise L looks and I denote the radar cross-section of the imaged surface [22–24]. An inherent feature of SAR images is the existence of speckle noise. Speckle noise is arbitrary and deterministic in an image [25]. Speckle noise degrades the quality of SAR images. Conversely, a radical decrease in resolution may be the main reason for poor effective perseverance.

Speckle is the impedance or declining shape. In a fully developed speckled image, the bright dots show where the impedance is constructive and the dark dots show where the impedance is destructive. The constructive and destructive impedance is shown and plotted in Fig. 9a–d.

3.2 Distribution of Speckle Noise in SAR Image

The factual properties of a speckle shape depended on 2 angles: the first on the intelligibility of incident light and the second on the dissipating surface information [26]. It is identified [24, 27, 28] that the foreseen power of a L-look SAR image prepared on the implicit reflectivity is gamma distributed [29, 30].

Fig. 9 Plotting bright and dark point of the speckled image
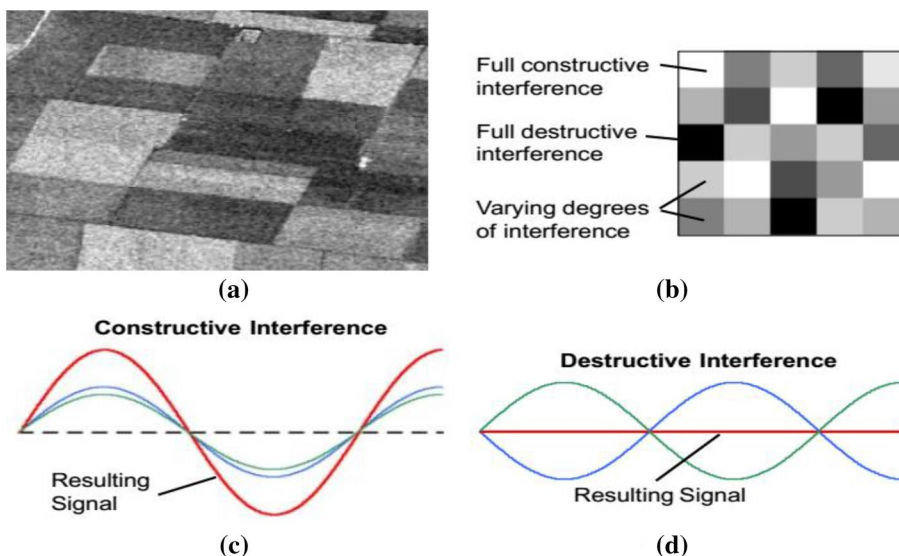
$$P(I|S) = \left(\frac{L}{S}\right)^L \frac{I^{L-S}}{\Gamma(L)} \exp\left(-\frac{LI}{S}\right) \qquad (2)$$

4 SAR image Despeckling Methods

A mass of despeckling filters, methods, and techniques can be acquired by linking the dissimilar domains of estimation (spatial, homomorphic, wavelet, and homomorphic-wavelet), A non-comprehensive evaluation and classification of approaches are presented in this section. The major literature related to Bayesian and non-Bayesian methods are discussed in this section. Figure 10 in this section depict the classification of various SAR image despeckling methods.

4.1 State-of-art Based SAR Image Despeckling

Some popular State-of-art based SAR image despeckling methods are discussed, below:

4.1.1 Bayesian Approach in Spatial Domain

Lee [1] in 1980 used the neighborhood intensity values in the kernel. All the pixels are processed separately. During the working of the kernel, local statistics of pixels within the kernel are estimated. Minimum Mean Square Error estimator (MMSE) calculates the weight function. This technique despeckles the speckle-noise with better precision but the minute details are deformed in the image. This originally first paper [1] contains the solution for both additive noise and multiplicative speckle-noise. It is purportedly the first-ever prototype-based despeckling filtering method [1]. Later the solution was systematically established in [2] and rectified in [3] embedded with the sigma filter. The Lee filter has a drawback of losing edge details as they left noisy after despeckling.

The Lee refined filter [31] in 1981 was intended to remove the demerit of remaining noisy edge boundaries left by Lee filter. In order to upgrade this filtering methodology, as 7×7 sliding windows are moved over a SAR image and edge is detected, then the system practices the local shield to evaluate its aspect. At maximum 8 edge-guided non-square masks are permitted. The local average and variance are evaluated and applied inside the local 7×7 mask which improves the edge aspect. If there is none of the edges is found, approximations are determined over the entire 7×7 frames. The major demerit of this filter is it only works using the fixed mask size 7×7.

The Frost filter [32] in 1982 is an exponentially weighted averaging filter and is adaptive in nature. An optimal MMSE filter is used the SAR images for smoothing. The speckle-noise is reduced by this filter and minute
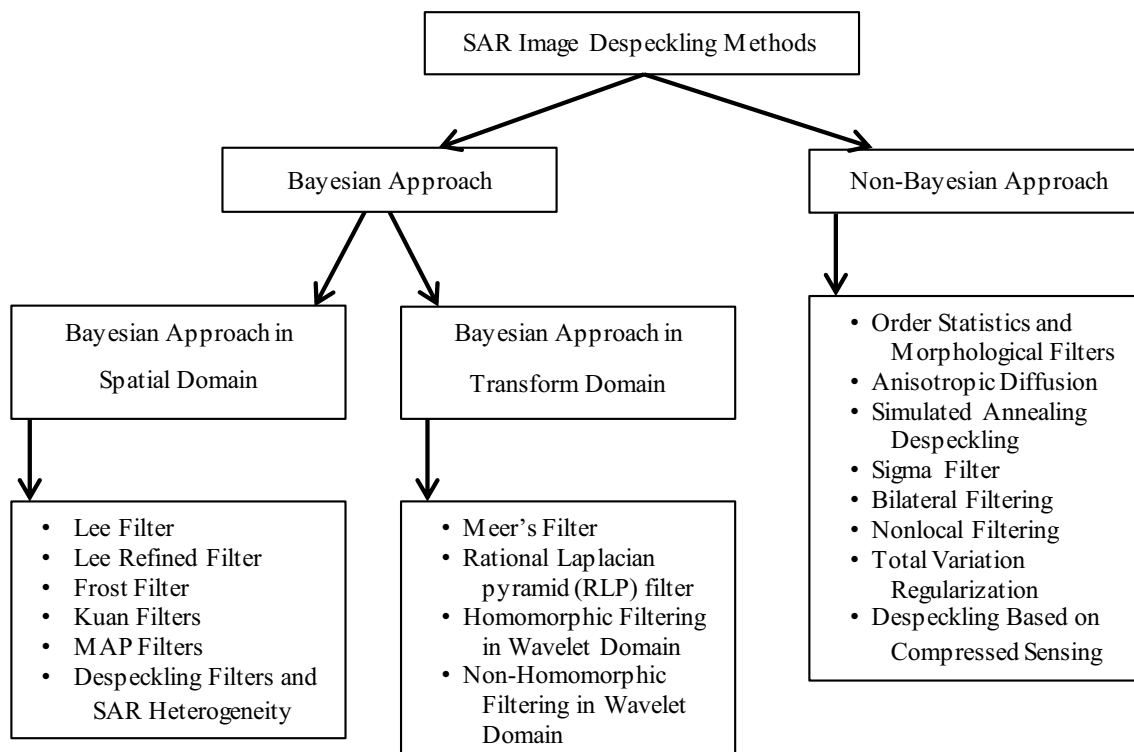

Fig. 10 Classification of SAR image despeckling methods

details are saved in the image. Its major demerit is blurriness in the output despeckled images. An ideal framework for the SAR imaging process is derived in [32] and smoothening is shown. The SAR imaging framework demonstrates that the SAR image is degraded by multiplicative speckle-noise. The framework leads to smoothing radar images using an optimum (minimum MSE) filter. The local block processing is applied here inside the homogeneous areas of the SAR image which preserves the edge and texture information and provides the minimum MSE value inside this region. This filter shows better computationally complexity and efficiency of this adaptive filter is qualitatively and quantitatively compared with several traditional filters using real and speckle added SAR images. With the advancement of time, there is no much advancement or development in the Frost filter either by researchers or others, except only some heterogeneity adjustments were made to all spatial Bayesian filters [33] by Kuan in 1985.

Kuan [33] in 1985 proposed a method based on the advancement of Lee's algorithm. It is a kind of adaptive speckle-noise smoothing filter. It is adapted to local alterations in image statistics related to a non-stationary average and variance image prototype. This filter has strengthened to manage various noises that rely on signal typical features. This filter is capable of smoothing the speckled SAR image whose speckle distribution and image statistics are unknown. Film-grain and Poisson signal-dependent restoration issues are also taken as examples. In addition, preceding information about the original image is also not needed. The disadvantage of Kuan filter is over the smoothing of fine details and the computational complexity of the algorithm is also very high.

Lopes [34] in 1990 analyzed the best-renowned filters. It is done by analyzing the experiments pertain to the variation local coefficients of the despeckled SAR image, which defines the heterogeneous region properties of the observed SAR image. Some applied benchmarks are then bringing together to it to adapt the filters in order to make them more well-organized and proficient. Later filters are verified on a speckled paired original SAR image and actual speckled SAR image. As it is believed, the new fresh innovative filters perform superior, i.e., it improves and smoothes the average fields uniformly and at the same time efficiently maintain texture and edge information, linear features, and point target responses.

The MAP filters prototype in the local domain is the C-MAP filter, brought in [35] in 1990 and exhaustively evaluated [36] in 1993. This method supposes that speckle-noise and the reflections of the radar signal together comply with Gamma distribution and calculates the MAP equation. This method intended to reduce and eliminate the speckle-noise while maintaining fine details and homogeneous and diverse areas in the image. The

dissimilar sizes of the filter alter the quality of filtered SAR images. If the filter is very small in size, then the speckle-noise filtering procedure is not efficient. In this method, the information of the images gets lost, if the filter is very large in size. A 7×7 filter size gives the greater trade-off.

4.1.2 Bayesian Approach in Transform Domain

Donoho et al. [37] in 1994 introduced a technique to retrieve the performance of undefined evenness from a speckled image. The Sure Shrink technique was introduced that eliminates the speckle-noise by performing the operation of thresholding on observed wavelet factors. The thresholding is adaptive: the degree of a threshold is assigned to each color resolution level by the fundamental of optimization the Stein Unbiased Estimate of Risk (Sure) for threshold determines.

Meer's filter [38] in 1994 considers a native neighborhood organized by three concentric sliding masks, 3×3, 5×5, and 7×7. A uniformity index is specified by Cg, calculated on every mask. The local mean over the highest mask fulfilling a uniformity standard, explained through thresholding its Cg, is specified like results. If this type of mask is not present, then Kuan's LLMMSE determines the innermost 3×3 masks allocated to the middle of a pixel. It is capable of restoring and maintaining point objects, linear features, and edges. It has the meritorious capability of shrinking its mask size. The execution of this filter is better on point objects and linear characteristics than Lee's refined filter that, still, far better on linear edges.

Guo et al. [39] in 1994 introduced a robust speckle-noise reduction method related to wave thresholding of the log-transformed speckled images. The computational cost of the method is low and it reduces the speckle-noise while preserving the fine details image. Both soft and hard thresholding methods are considered.

Donoho [40] in 1995 proposed the method for recreating an undefined function f from noisy data by giving the classical hard and soft thresholding method. The work presented in [40] one of the pioneer's works in the field of image denoising. The rearrangement process is stated in the wavelet domain by interpreting all over the experimental wavelet factors.

Gagnon [41] in 1997 proposed a wavelet-based despeckling method grounded on Symmetric Daubechies. The speckled wavelet coefficients are modified by the shrinkage principle and restore the filtered image. It uses the concept of the elliptical soft thresholding method. The speckled image is directed to log transform followed by N level transform and then its covariance and mean is evaluated. Then inverse wavelet transform and exponential transformation

are performed. The method reduces the speckle-noise efficiently, but the computational load is increased.

Aiazzi [42] in 1998 applied an adaptive smoothing filter to the various perseverance of the Laplacian pyramid of a speckle SAR image. In the case of real speckled SAR images, every level is regarded by Signal to Noise Ratio (SNR) that rises as the perseverance gets reduced. The hypothetical based theoretical framework is established for SAR image-dependent speckle-noise models. A rational Laplacian pyramid is engaged to deal with multiplicative speckle-noise. The experimental results are shown on gray-level SAR images degraded by real and replicate noise. Later improved by Aiazzi [43] in 1998, here ratio Laplacian pyramid (RLP) is presented to compare speckled SAR image dependency behavior speckle-noises. The local statistics filtering mechanism is enforced to various local perseverance of the RLP of a speckled SAR image. Also, the reckoning of the spatial statistics operating this method is more precise to the multi-perseverance model. The objective of this filter is to reduce the speckle-noise until smoothing the homogeneous regions and preserving fine details. An adjustment, although, going to be arranged on the textured region. This method is a complete procedure is set up, and a common technique, where the speckle-noise differences are impractically obtained at each resolution, is developed.

Hervet [44] in 1998 presented a detailed investigational assessment of representative filters from both groups i.e. spatially adaptive filters and wavelet techniques. Here the spatially adaptive statistical filter gives improved despeckling and preservation of details than wavelet-based techniques. But the wavelet-based techniques have specific advantages related to statistical filters that are not spatially adaptive.

Sveinsson et al. [45] have given 2 wavelet transformations despeckling method for SAR image. First, it is made use of DWT overall filter banks. This oversampled DWT is known as double-density DWT (DD-DWT). Second, a DWT related to two dual real wavelet trees is applied. The despeckling technique offered demonstrates the abundant potential for despeckling and, later, able to deliver idle detection performance for SAR-based detection.

Solbo et al. [46] in 2004 presented the homomorphic wavelet utmost a rational filter and a wavelet related statistical speckle-noise reduction filter equivalent to renowned/spl Gamma/-MAP filter. The log transform is applied so that speckle-noise can be added to nature and statistically free the radar cross-section. Additionally, it is proposed to practice the general inverse Gaussian distribution like a general prototype for the wave coefficient for both the inverse image and the speckled noise image. There is information near to impractical prototype than the additive speckle denoised with some other filters to the speckle-noise eliminated by the homomorphic/spl gamma/-WMAP filter. The wavelet

despeckling technique related to Bayesian shrinkage preserves the edge details is proposed by Dai [47]. The speckle-noise-free wavelet factors are projected from Bayesian wavelet compression factors. Edge details are gained using an improved ratio edge detector. This acquired detail is later used in the speckle-noise reduction processes to retain edges.

Bhuiyan et al. [48] in 2005 introduced a modern homomorphic Bayesian wavelet related least average novel error filter of speckle-noise reduction in SAR images. The wavelet coefficient and the speckled SAR image of the logarithmically changed reflection image are prepared to make use of Cauchy prior and an additive white Gaussian noise distribution. This prototype is previously used to design a Bayesian least average absolute error analyzer. The experimental results are tested on the classic speckle-noise-free image reduced with mock speckle-noise and an original speckled SAR image, and consequences explain that performance of this method that is greater to other prevailing approaches regarding PSNR, smoothness in the identical regions and despeckled image visual appearances. Later this work was enhanced by Bhuiyan et al. [49] in the year 2007 by introducing the latest spatially adaptive wavelet related Bayesian techniques for reducing the speckle-noise in SAR image. The wavelet factors of logarithmically changed reflection and speckle-noise are formulated reciprocally to make use of zero-space Cauchy and zero-mean Gaussian distributions.

Wu [50] in 2010 proposed a method that performs an amalgamation of wavelet and curvelet soft estimating techniques after that it calculates the variance amid the gained two images. This mechanism is proficient enough to restrain the speckle-noise efficiently and preserves the fine details such as edge, texture, etc. of the image. The main disadvantage is that it produces blurriness. In the same year, Jennifer Ranjani et al. [51] introduced DTCWT based SAR image despeckling that considers the major requirements of the wavelet factors across different scales. This has the advantage of improved directional selectivity, approximate shift-invariance and complete reconstruction over DWT. In each and every sub-band the wavelet coefficient of the DTCWT is prototyped with a bivariate Cauchy PDF that adapts the statistical reliance between the wavelet factors. The 2-D Mellin transformation derives the backscattered elements of the bivariate Cauchy before noise considerations. This technique is faster and operative when equated with other previous methods of experimental integration.

Vijaykumar [52] in 2012 proposed a dual-tree complex wavelet transform (DTCWT) related to SAR images speckle-noise reduction technique which is a function in interscale and intrascale requirements of DTCWT. A multivariate Cauchy PDF is in a job to apply the outer scale and inner scale dependencies of the wavelet factors in every sub-band. This technique uses the average and directional median values of the relative mask to estimate the outer scale and

inner scale dependence vector of the wavelet factors. The 2-D Mellin transform derives the dispersion parameter of the multivariate Cauchy prior. In the same year, Tao et al. [53] introduced a novel Contourlet-based regularization technique to eliminate speckle-noise without introducing artifacts. The elimination of speckle-noise is significant and structures of the scene are well preserved. The experimental results prove such dominance on real SAR images. In 2012, Argenti et al. [54] introduced a despeckling SAR image technique using undecimated wavelet transform and the MAP principle. The MAP solution is based on the hypothesis that wavelet factors have an identified scattering. The computational cost is reduced which was the major drawback of using the GG distribution. In 2012, Chen et al. [55] introduced a stationary-wavelet-related speckle-noise reduction mechanism based on the two-sided common gamma distribution model. The model has low computational cost and decent quantitative values. It preserves the structural details and also reduces the speckle-noise effectively.

4.1.3 Non-Bayesian Approach

Perona et al. [56] in 1990 introduced a concept of anisotropic diffusion and proposed a modern approach of scale-space and a class of procedures used to understand the diffusion method is known. This technique is extensive in image processing. The primary goal of this technique was to despeckle the image noise and preserving the image minute details such as line, edge and other details, etc. that help in the understanding of the image. Yu et al. [57] in 2002 smartly fitted the concept of anisotropic diffusion [56] reducing the speckle-noise and applied it to the coherent images. This research shows greater execution as per average preservation, despeckling, and edge determination. The performance is better than traditional methods and conventional anisotropic diffusion method. Yu et al. [58] in 2004 introduced a prominent application for coastline detection using the despeckling related to anisotropic diffusion.

The bilateral filter, originally familiarized by Tomasi et al. [59] in 1998 for gray-scale images, which is extended in recent times in the area of SAR images despeckling by Zhang, et al. [60] in 2011. A bilateral filter is a non-linear, smoothing, fine detail (edge, line and texture preservation) preservation method, which reduces noise for degraded images. This replaces the intensity of each and every pixel with the intensity of the weighted mean values from the nearest pixel. The adaptive version of bilateral filter appropriate in SAR images despeckling is proposed by the Li et al. [61] in 2013, the spatial weighting is a Gaussian operation whereof duration rests on the topical factor of variation, which is equivalent to the modified Frost filter.

Mastriani et al. [62] in 2004 introduced an enhanced directional smoothing (EDS) method for SAR images edge-preserving filtering. The EDS removes speckle-noise from SAR images without distorting or disturbing edges. This modern filtering technique is proved effective by associating with popular speckle-noise reduction techniques on SAR noisy images. The EDS algorithm delivers greater execution in assessment to the classical filters with regards to smoothing homogeneous region and preserving the fine details such as edges and characteristics. The ability of the method stimulates the possibility of using the method in a number of ultrasound and radar applications. Furthermore, the method is computationally effective and the ability to reduce noise while preserving some fine details of the real image.

Buades et al. [63] in 2005 proposed a new technique, 'method noise', to estimate and give an account of the performance of digital image denoising approaches. In this paper, firstly the method noise is computed and analyzed to various denoising procedures, namely the local smoothing filters. Secondly, a new nonlocal means (NL-means) algorithm is proposed which is grounded on the nonlocal mean of all pixels in an image. Finally, the NL-means mechanism and local smoothing filters are experimentally matched.

Achim [64] in 2006 suggested an adaptive MAP analyzer with a heavy-tailed Rayleigh signal framework. The multiplicative behavior of speckle-noise is changed into additive by executing the log transform. Here the original and imaginary parts are explained by an alpha-stable group of distributions. There is another statistical theory that relies on the Mellin transform method, is applied to evaluate the framework elements from noisy translations.

Sparse prototypes are based on compressed sensing recommended by Donoho [65] in 2006, which is a depiction of signals with multiple patterns at a sub-Nyquist rate. A new signal description prototype has lately occurred highly extensive and has captivated the consideration of researchers who are working in the field of real image formation which is distorted by additive noise also in different other fields. After that, a few speckle reduction techniques related to shrank sensing model and thin image have become visible [66–68].

Lee et al. [69] in 2009 extended and advances the Lee sigma filter [70] by eliminating its drawbacks i.e. blurring effect, disappointing solid reflected targets, and biased estimation. The bias adversity is resolved by reconsidering the sigma range related to the probability density function of the bias noise. To resolve the difficulties of blurring effects and disappointing solid reflected scatterers, a target signature preservation method is established.

Teuber et al. [71] in 2012 proposed a basic parity volume and non-spatial filter for SAR images degraded by multiplicative noise. The measured filters are a simplification of non-spatial mean filters of Budess [63], which is well identified to remove additive Gaussian noise. At last, the

restoration outcomes for coherent images degraded by multiplicative Gamma and Rayleigh noise are validating the better execution of these non-spatial filters has been offered. Gragnaniello et al. [72] in 2012 provided some vision in the perspective of types related nonspatial filtering by performing dummy tests in a streamlined condition. Then recommends an absolute kind of the SAR-BM3D speckle reduction mechanism in which each and every pixel is first groped as uniform or not, and then filtered with the class-adapted framework. While outcomes on original SAR images are still uncertain, earlier some valued improvements in specific regions that draw attention to this technique.

4.2 Recent Trends of SAR Image Despeckling

Some recent popular SAR image despeckling methods are discussed, below:

4.2.1 Bayesian and Non-Bayesian Hybrid Approach

Christy [73] in 2013 introduced an enhancement principal of the Non-Local Means Filtering (NLMF) technique. A deformation adaptive non-local means filtering (DA-NLMF) is proposed that implements a discrete adaptive weighting function preserving edges and other granular information that is greater than non-local means. DA-NLMF is used for SAR image despeckling as a significance sampling Unscented Kalman filter (ISUKF) as well as a resource post-processing process. This combination of (ISUKF and DANLMF) gives an adept despeckling result. In the same year, Heng-Chao Li [74] proposed a modern Bayesian multiscale method for SAR images despeckling technique in non-homeomorphic plans. In order to deal with multiplicative speckle-noise, linear dissociation is applied for the speckle addition. After that in SWT, the 2-way normal gamma distribution is known as before, in order to deal with heavy-tailed disposition of the wavelet factor of speckle-free reflectivity. The compression rules used are threshold on the diagonal element of the image that causes the horizontal and vertical element to be unfiltered hence the speckle-noise reduction process has a high scope of improvement.

Sethunadh et al. [75] in 2014 developed a modern adaptive SAR image speckle reduction process in the local domain applying statistical inter-scale dependence of nonspatial transform factors; the task is greater adept in preserving the lager structured area. Lei Zhu [76] in 2014 identified the detail-preserving anisotropic diffusion (IDPAD) has been introduced for the SAR image that experiences a primely low speckle reduction presentation at the edges and severe blocking artifacts in a similar region.

Sara Parrilli [77] in 2012 introduced a speckle reduction method related to wavelet shrinkage and non-local filtering by applying probabilistic correspondence estimate. The outcomes are constant with PSNR values showing greater structure preservation and despeckling. In addition, the mechanism has greater smoothing strength in the corresponding region. Additional essential non-local filtering related Bayesian frameworks have been introduced in [78] that have been analyzed on both ultrasound [79] also SAR images [80]. This work presents the capability of non-local average filtering in the area of speckle reduction.

David de la Mata-Moya et al. [81] in 2014 introduced a SAR image despeckling technique grounded on empirical mode decomposition. The work calculates a new threshold value with a sliding mask to preserve the minute details i.e. edges, texture and despeckling [82]. The outcomes display an acceptable despeckling avoiding an over-smoothing in the whole image.

Yao Zhao et al. [83] in 2015 introduced a dual-formulation related Adaptive Total Variation (ATV) ordering technique which is executed to describe the Total Variation ordering. Parameter optimization of the total variance ordering is accomplished at the noise level evaluated through wavelets. The designed mechanism gives a great advancement in comparison to the earlier standard total variance technique regarding despeckling in identical regions and detail preservation in diverse regions, but even then, sometimes the generation of blocked artifacts is found. Some of the variational based despeckling works that are grounded on total variation regularization are discussed in [84–88].

Abdourrahmane Mahamane Atto [89] in 2016 presented a paper, which gives statistical features of waving carriers when thought is capable of realizing as a deterministic slice-wise regular function (signal) and multiplication of a constant random field (noise). This multiplicative monitoring model is evaluated in two standard frameworks, (1) direct wavelet transform of the model (2) log transform of the model prior to wavelet degeneration.

Diego Gragnaniello [90] in 2016 framed a recent method for synthetic aperture radar despeckling, establishing the adjustment of different alternative evaluations of the identical information. They have given a reliable pixel-wise categorization of an image; so that we can take advantage of this diversity by choosing the most appropriate amalgamation of values for each image region. Using this approach enhanced an algorithm where only two modernizing despeckling techniques, characteristic of favorable features, are added linearly.

In 2019, authors of [91] proposed a model where Multi-Objective Particle Swarm Optimization (MOPSO) is used for despeckling a SAR image in Dual-Tree Complex Wavelet Transform (DTCWT) domain. This work performs well in terms of visual results and also in performance metrics of results.

In 2018, authors of [92] attempts to address non-fixed spot decrease in high-resolution synthetic aperture radar (HR-SAR) images, utilizing a novel Bayesian methodology. From the earliest starting point, non-fixed spot is depicted. Second, an innovative log-normal mixture model (Log-NMM) is proposed to model the focal information; the information priors are tended to by utilizing Fields of Experts (FoE); and then the despeckling model is settled in danger to MAP methodology. The exploratory outcomes show that the recommendation passes on top level despeckling execution on synthetic and genuine HR-SAR information, and show that the spot is non-fixed in the HR-SAR information of intrigue.

In 2019, authors of [93] make the robotized moved image methodology a hazardous errand. Appropriately, diminishing of spots is a basic pre-handling step. The decision of bit channel relies upon the necessities of an application and the attributes of the dataset. In this appraisal, some most favored spot channels are outlined for the information from Sentinel-1 to portray degree. The Sentinel-1 (VV-vertical transmit, vertical get and VH-vertical transmit, level get) polarizing channel information were utilized to layout AI checks, unequivocally, random woods (RF) and strengthen vector machine (SVM), to depict a submerged area. The correctnesses of the depictions were surveyed by kappa coefficient, when in doubt exactnesses, and maker's and client's correctnesses. The stream assessment recommends a way to deal with oversee direct screen harm and give head data to enable neighborhood structures to manage water-related hazard, land organizing, water the administrators, and flood control programs.

In 2017, authors of [94] proposed a methodology (Guided SAR Image Despeckling with Probabilistic Non Local Weights) replaces parametric constants subject to heuristics in GGF-BNLM system with logically picked characteristics dependent on the image estimations for weight tally. Proposed changes make GGF-BNLM structure flexible and in like manner, essential improvement is made like execution. Exploratory evaluation on SAR images shows mind passing spot spoil without trading over region security when stood isolated from GGF-BNLM technique. Results are also detached and other cutting edge and phenomenal SAR depseckling systems to show the plentifulness of the proposed technique.

In 2019, authors of [95] proposed a method for despeckling of SAR image contains two phases. First stage is despeckling process which depends on directional smoothing and hard thresholding structure and second stage is picture update process which depends in the wake of applying Hybrid Laplacian Gaussian channel. The proposed work has been endeavored and show crucial execution over the current structure. The reenactment results validated that accomplishing a predominant Peak Signal than Noise Ratio (PSNR),

Speckle Suppression Index (SSI) secluded and existing framework.

In 2017, authors of [96] present another structure where another nonlocal sparsity key term knows about work with the essential term obviously. To get the two nonlocal sparsity fundamental terms, we outline the picture into various sorts as appeared by the quantifiable properties of spot in SAR picture unmistakably off the bat. By at that point, they pick the best methodology to denoise various sorts of picture and use the predicted coefficients of these denoising results to survey the nonlocal sparsity basics. Our system not just changes the well-salgortudied methodology for CSR, yet what's more appusing applialgories to despeckle SAR picture. Starter results, did on both reenacted SAR images and genuine SAR images, show that the proposed approach has a certifiable despeckling execution to the degree both assessment pointers and visual quality evaluation.

In 2016, authors of [97] proposed MAP despeckling technique subject to directionlet transform. To improve the denoising execution, they join the intra-scale reliance to the degree introduced data to the MAP estimator to refine the evaluated outcomes. At long last, we separate the proposed check and a couple of other spot channels applied on synthetic and authentic SAR images. Fundamental results show that the proposed methodology outsmarts different channels the degree that sign to-noise degree, edge security and badly characterized number of looks checks all around.

In 2019, authors of [98] proposed another cross assortment despeckling framework, considering MAP estimator and non-local PCA in wavelet domain. This framework was separated and some top level despeckling methods. The exploratory outcomes showed that the proposed system prompts an unmatched spot decrease in homogeneous regions while making sure about subtleties.

4.2.2 Deep Learning Based Despeckling

In 2019, authors of [99] proposed a deep learning based down to earth approach to manage administer despeckle synthetic aperture radar (SAR) images without using ground truth (despeckled images). Results have been driven on ImageNet dataset additionally as on the genuine SAR images. The results are bore witness to both truly similarly as quantitatively and isolated and front line moves close.

In 2017, authors of [100] proposed the intensity of deep totally convolutional, an encoding-unwinding structure for multisource SAR picture despeckling. The structure contains an advancement of convolution and deconvolution layers, confining a through and through non-direct mapping among noise and clean SAR images. With enlargement of skip association, the structure can keep picture nuances and accomplish the methodology for residual learning which

deals with the notorious issue of vanishing inclinations and reestablishes blend. The starter results on replicated and veritable SAR images show that the introduced approach achieves redesigns in both despeckling execution and time proficiency over the front line despeckling systems.

In 2019, authors of [101] analyzed the steady advancement in image despeckling, unequivocally fix based nonlocal confining and deep learning techniques. These two get-togethers of structures offer relating properties at any rate have not yet been joined. We explore frameworks to profit at any rate much as could reasonably be normal from each approach.

In 2019, authors of [102] proposed the usage of a cost work considering both spatial and quantifiable properties. Actually two wrinkle: rout the trade off between spot spread and nuances veil; find a sensible cost work for despeckling in solo learning. The figuring is grasped on both authentic and reenacted data, demonstrating flabbergasting grandstands.

In 2019, authors of [103] proposed despeckling of Synthetic Aperture Radar (SAR) data using deep convolutional structures. Key outcomes displayed promising results using synthetic and veritable images.

In 2019, authors of [104] inquired about the usage of deep learning to improve nonlocal despeckling. They use plain non-iterative nonlocal infers despeckling, with loads gave, for each estimation window, by a fittingly planned deep CNN. Evaluations on synthetic and authentic SAR data show in this way to supervise beat normal nonlocal systems.

In 2019, authors of [105] proposed convolutional neural frameworks based estimation for despeckling. The structure is set up on reenacted SAR data. The paper is generally spun around the use of a cost work that surveys both spatial consistency of picture and quantifiable properties of noise.

In 2020, authors of [106] proposed a novel two-fragment deep learning (DL) compose with the noise issue. In any case, the surface estimation subnetwork is made to pass on TLM, which surveys the randomness and size of the surface scattering. By then, the noise takeoff subnetwork learns a spatially factor mapping between the noise and clean images with the help of TLM. Right when the structure has been readied, it can normally gauge the surface part and wrap up whether to smooth the local noise or keep up the detail. Comprehensive assessments on reenacted and bona fide SAR images show the better execution of the proposed strategy over the top level frameworks with concession than both the refreshed perception and quantitative evaluation.

In 2017, authors of [107] proposed a deep-learning-based methodology for image despeckling convolutional neural structure (ID-CNN), for normally expelling spot from the data noisy images. In particular, ID-CNN uses a great deal of convolutional layers near to assemble normalization and balanced straight unit establishment work and a piece savvy division residual layer to check spot and it is set up in a

through and through structure using a mix of Euclidean trouble and complete assortment distress. Clearing evaluations on synthetic and veritable SAR images show that the proposed strategy achieves noteworthy updates over the cutting edge spot decline systems.

In 2018, authors of [108] proposed a noise-invariant CNN that uses regularization for keeping part courses of action acknowledged by this noise. Before CNN getting ready, they performed SAR picture despeckling using the improved Lee sigma channel for merge extraction. By then, they made SAR images for CNN getting ready by adding contact noise to the despeckled images. The regularization improves both the area constitution to spot noise and SAR target acknowledgment. Starters on the moving and fixed objective obtaining and acknowledgment database show that the proposed CNN notably improves the party precision isolated and the standard methods.

In 2018, authors of [109] proposed a novel deep neural system structuring unequivocally got ready for despeckling reason. It utilizes a convolutional neural system to remove picture joins and change a discrete RCS PDF. The structure can be set up by either completely imitated picture patches or genuine SAR images. The outcomes show the plentifulness of the proposed despeckling neural system separated and three forefront channels.

5 SAR image Despeckling Performance Measures

In SAR image despeckling, the utmost thought-provoking job is the speckle noise reduction by preserving the fine details of the image. The most evident concern in this field is the speckle-free reflectivity that is unidentified as the ground truth is unknown. Another significant matter is the relationship between quality and reliability of despeckled SAR images. The other despeckling outlines i.e. feature and reliability of originality of despeckled SAR images is calculated by analyzing the degradation in the homogeneous regions, i.e. reduction of speckle noise and preservation of fine details in heterogeneous areas. Visual inspection of despeckled SAR image is one methodology for the assessment of quality of the image. However, Performance metrics for SAR image analysis, can be analysed by with–reference and without–reference indexes [110, 111].

There is an infinite literature available in the field of image denoising and despeckling in the presence of the reference image. In this case the author has complete information about the image. In the case of with-reference index, the image researchers can easily compare their despeckling results with the reference images. It creates the opportunity to enhance the results as the previous statistical details are available [28, 64, 112, 113].

5.1 With-Reference Indexes

Some of the major performance metrics using with reference indexes, are give below:

Performance measures	Mathematical formulation
Mean square error (MSE)	$MSE = E[(\hat{f} - f)^2]$, where $\hat{f}, f$ are the despeckled and speckle free images
Structure Similarity Index Metric (SSIM) [114]	$SSIM(a,b) = \frac{(2\mu_a\mu_b + P_1)(2\sigma_{ab} + P_2)}{(\mu_a^2 + \mu_b^2 + P_1)(\sigma_a^2 + \sigma_b^2 + P_2)}$ where, μ_a, μ_b, σ_a, σ_b and σ_{ab} are the local means, standard deviation and cross variance for images x; y. $P1 = (0.01 * L)^2$ and $P2 = (0.03 * L)^2$,
Signal to noise ratio (SNR)	$SNR = 10.log_{10}\left[\frac{Var[g]}{MSE}\right]$ where, $Var[g]$ is speckle free image variance
PSNR	$10log_{10}\left(\frac{255 \times 255}{MSE}\right)$
Energy signal-to-noise ratio (ESNR)	$ESNR = 10.log_{10}\left[\frac{E[f^2]}{MSE}\right]$ where, $E[f^2]$ is the speckle free image power
Universal image quality index (UIQI)	$Q = \frac{\sigma_{xy}}{\sigma_x\sigma_y} \bullet \frac{2\bar{x}\bar{y}}{(\bar{x})^2 + (\bar{y})^2} \bullet \frac{2\sigma_x\sigma_y}{\sigma_x^2 + \sigma_y^2}$
Feature similarity index metric (FSIM) [115]	$FSIM = \frac{\sum_{a\in\Omega} Z_L(a).PC_m(a)}{\sum_{a\in\Omega} PC_m(a)}$ where Ω signifies the spatial transform of the complete image [116]
Edge correlation (EC) index [117] [118]	$EC = \frac{Cov[f^H\hat{f}^H]}{\sqrt{Var[f^H].Var[\hat{f}^H]}}$ $f^H, \hat{f}^H$ are the high pass smoothed noise-free and denoised images
Pratt's figure of merit (FOM) [119] [120]	$\frac{1}{max(\hat{P},P)}\sum_{m=1}^{\hat{P}} \frac{1}{1 + d_m^2 \alpha}$ $\hat{P}, P$ is the no. of pixels belonging to an edge in denoised SAR image patches and noise-free clean image patches. d_m^2 is the Euclidean distance between the edge pixels in the denoised SAR image patch and nearest ideal edge pixel in the clean SAR image [120]

5.2 Without-Reference Indexes

Some major performance metrics for without reference indexes, are given below:

Performance measures	Mathematical formulation
Equivalent number of looks (ENL) [121] [122] [123]	$ENL = \left(\frac{\mu}{\sigma}\right)^2$ where, μ is mean and σ is variance of image
Important information both in homogeneous and non-homogeneous areas [24]	$R(m) = \frac{a(m)}{\hat{b}(m)}$ where, $a(m)$ is the speckled image and $\hat{b}(m)$ is the despeckled image
Coefficient of variation (CV)	$CV = \left(\frac{\text{Standard deviation}}{\text{Mean}}\right) \times 100$
Target-to-clutter ratio (TCR) [124, 125]	$TCR = 20log_{10}\frac{max_{pp}[g]}{E_{pp}[g]}$ where, pp is the patch that contains the objective point and max_{pp}; E_{pp} are computed over that patch
Noise Variance (NV) [126]	$\sigma^2 = \frac{1}{N}\sum_{j=0}^{N-1} u_j^2$ where, N is the size of the image

6 Comparison of SAR Image Despeckling Methods

For relative study of SAR image despeckling methods, the experimental results of some existing conventional and non-conventional methods are analyzed using two aspects: (1) qualitative study by analyzing the visual appearance of the despeckled SAR image, and (2) quantitative study by analyzing the performance metrics. The quality of despeckled SAR image can be analysed by visual appearance and also by evaluating the quantitative values. In order to perform to qualitative analysis there is no mathematical or precise method available in the literature. For better visual inspection of despeckled SAR image, usually, there are six criteria are followed: (1) reduction of granular structured speckle noise; (2) visibility of the artifacts; (3) preservation of fine details like edges in the heterogeneous areas; (4) visibility of low contrast objects; (5) smoothness in homogeneous areas, and (6) preservation of the texture. The accuracy of SAR image despeckling techniques are measured by some standard performance measures, such as: Noise Variance (NV), Mean Square Error (MSE), Equivalent Number of Looks (ENL) and Coefficient of Variation (CV).

6.1 A comparative study

The experiments were conducted on several real speckled SAR image acquired from public access database (http://www.sandia.gov/RADAR/imagery/https://photojournal.jpl.

Table 2 NV, MSE, ENL and CV of despeckled SAR images

Filtering methods	Performance assessment parameters			
	NV	MSE	ENL	CV
Real speckled SAR image (see Fig. 11)	7.2567	–	1.8055	32.6373
[32]	6.3378	841.8739	2.3461	34.9981
[33]	6.0981	913.8233	1.9091	36.2341
[22]	5.0002	689.0156	2.5058	31.9958
[76]	5.2134	795.2331	2.1089	33.4568
[39]	5.0024	623.2301	1.6728	33.8211
[81]	4.9671	699.8975	2.0191	35.7294
[37]	4.997	681.1221	2.1741	35.7912
[51]	0.9025	980.1683	2.4281	33.9510
[52]	0.5632	1001.0281	2.5601	34.2325
[83]	0.4561	984.0909	2.5229	34.1919
[77]	0.42123	876.9622	2.0019	33.4227
[82]	0.4668	976.9123	2.5332	33.7213
[125]	0.4084	890.2846	2.4928	35.9696
[63]	0.4001	925.6580	2.5028	34.0819

Fig. 11 Real speckled SAR image

nasa.gov/catalog/PIA01763 http://eo.belspo.be/). But here in the article, the experimental testing is performed on Fig. 11.

From the experimental results and analysis, it is found that Bayesian methods in spatial domain removes the speckle noise efficiently but the fine details gets blurred and sharp edges gets distorted in SAR images. On the other hand, the Bayesian methods in transform domain and non-Bayesian methods are capable enough to preserves the fine details of the SAR image while reducing speckle content too. The accuracy and efficiency of the prevailing SAR image despeckling methods for analysis are based on the quantitative values of the performance metrics. The average results of some prevalent SAR image despeckling methods are shown in Table 2. The main factors that are analyzed in the despeckled SAR images are reduction of speckle noise, preservation of fine details, smoothness in the homogeneous areas and texture preservation in the heterogeneous areas. Therefore those performance parameters are selected for analyzing the quality of despeckled SAR images that covers the above discussed main factors that best describes the SAR image. The summary of some SAR image despeckling methods are briefly discussed in Table 3.
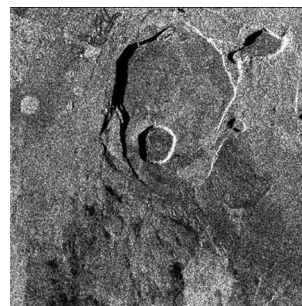
The NV value of the real speckled SAR image shown in the Fig. 11 is 7.2567. A mask of 25×25 is rotated on the image in a non-overlapping fashion, ENL value is calculated for each mask. Later average of all ENL value is evaluated that is equal to 1.8055. Its CV value is 32.6373. Frost et al. [32] and [33] reduces the speckle content from the image but it leads to introduction of impairments specifically more in [33]. Chen and Liu [22] and [76] are more efficient in reducing the speckle noise than the previous works. The texture in the heterogeneous areas is well reserved in the [22] and [76] but fine details are distorted in the [22] and artifacts are seen in the despeckled image of [110]. The smoothness in the homogeneous areas is well maintained in the [22] than [76]. The average difference between despeckled image and real SAR image is maximum in [33] among the [22, 32, 33] and [76]. Guo et al. [39] presents the despeckling results of soft and hard thresholding using DWT. The soft [39] is more efficient than hard [39] in terms of speckle reduction and smoothness in the homogeneous areas while the texture part in the non-uniform regions is well preserved in both the cases. The despeckling results of [81] and [37] are approximately same in terms of all quality factors but the computational cost of [81] is better than the [37].

The speckle content observed in the despeckled SAR images in [51, 52, 63, 77, 82, 83, 126] is highly reduced. Out of these, [63] is best in speckle reduction. Even the smoothness in the uniform regions is well maintained in these mentioned works. The average difference between despeckled SAR image and real speckled SAR image is maximum in [52]. The fine details are well preserved in the mentioned works. Out of these, [51] shows the minimum introduction of the artifacts. The computational cost of [52] and [63] are high.

Table 3 Summary of some SAR image despeckling methods

Despeckling methods	Advantages	Disadvantages
[32]	Smoothens the homogeneous areas, preserves edge structure, computationally efficient, effective in spatial domain	Ineffective in frequency domain
[33]	Deals with various types of signal-dependent noise, no a priori information about the original image are required, Simple structure of algorithm	Introduction of artifacts
[22]	It gives better results than the conventional wavelet thresholding algorithm, preserves edges	Kills too many wavelet coefficients that might contain useful image information
[76]	Preserves edges, improves the despeckling ability along the edge directions, no blocking artefacts in homogeneous regions	Over smoothening of homogeneous areas
DWT with Hard Thresholding [39]	An efficient selection of Change basis and Change level can improve and deliver the best results in terms of speckle reduction and smoothening	A big threshold leads to a large bias of the estimator; a small threshold increases the variance of the smoother
[81]	Preserve edge information discarding the noise, avoids over-smoothing in the whole image	Losing small structural features in the image
[37]	Recovers the unknown smoothness from speckled sampled data, it suppresses noise by thresholding the empirical wavelet coefficients, adaptive in nature	Better results depend on the underlying function that has jump discontinuities on a smooth background
[51]	Improved directional selectivity, approximate shift invariance, and perfect reconstruction over the DWT, faster and effective when compared to that of the earlier techniques on numerical integration	Noise near the edge left due to improper interdependences between a coefficient and its other neighbors
[52]	Efficient speckle reduction in in homogeneous regions, better despeckling performance and edge preservation capability	High computational cost
[83]	Eliminates undesirable detail whilst preserving the fine details such as edges, smooth the noise in homogeneous areas, even at low SNR's	Introduction of artifacts of "ghost" textures which do not exist in the reference images
H-BM3D [77]	Significant speckle reduction, no introduction of artifacts or any pattern in the despeckled images	Losing small structural features in the image
H-PPB [77]	Significant speckle reduction, despeckled image looks more pleasant than the others	Introduction of widespread artifacts resembling watercolor strokes
Coarse filtering [82]	Significant speckle reduction ability, preserves the fine details of the despeckled image	Introduction of artifacts
Refined filtering [82]	Low computational cost, reduces the artifacts generated in the coarse filtering stage using wavelets [82]	Inefficient for polarimetric SAR despeckling which is also a hot topic in SAR image processing
[126]	Supresses the speckle noise and preserves the edges	Sometimes over smoothening at the flat regions
[63]	Improved post-filtering clearness and a smaller amount loss of detail in the image compared with local mean algorithms	High computational cost

7 Conclusions

The speckle reduction in SAR images is one of the hottest topics in SAR image processing. The SAR images are inherently speckled in nature, but the main reason is constant interaction of the transmitted high-frequency radar waves with target areas. The speckle noise can be reduced or eliminated using suitable despeckling methods. Therefore, despeckling should be implemented to enhance the SAR image quality for more accurate pre-processing. This article discusses some of the most prevalent articles with their advantages and disadvantages. In order to deal with speckle noise, an efficient despeckling process requires a prior information about the noise map, adaptability and pattern distribution. The final objective of SAR image despeckling method is to obtain edge preserved despeckled images with reduced speckle content, smoothness in the homogeneous areas, preserved texture in the heterogeneous areas and no artifacts generation. This paper summarizes the SAR images, noise in SAR image i.e. speckle noise, SAR image despeckling methods. The comparative analysis of some recent methods and also some state-of art methods are analysed with their merits and demerits. This analysis of speckle noise will surely help to the researchers for developing new SAR image despeckling algorithms.

Compliance with Ethical Standards

Conflict of interest The authors of this research article declares that no conflict of interest in preparing this research article.

Consent for Publication All the authors of this paper have shown their Participation voluntarily.

References

1. Lee JS (1980) Digital image enhancement and noise filtering by use of local statistics. IEEE Trans Pattern Anal Mach Intell PAMI-2(2):165–168
2. Lee J-S (1981) Speckle analysis and smoothing of synthetic aperture radar images. Comput Graph Image Process 17(1):24–32
3. Lee J-S (1986) Speckle suppression and analysis for synthetic aperture radar images. Opt Eng 25(5):636–643
4. Translation Bureau (2013) Radar definition. Public Works and Government Services Canada
5. McGraw-Hill dictionary of scientific and technical terms. (1976) Daniel N. Lapedes, editor in chief. New York; Montreal : McGraw-Hill,[xv], 1634, A26 p
6. Abbreviations and acronyms. Navy dot MIL. United States Navy. Retrieved 9 August 2017
7. Small and Short-Range Radar Systems. CRC Net Base. Retrieved 9 August 2017
8. Real Aperture Radar. Available at: http://wtlab.iis.u-tokyo.ac.jp/~wataru/lecture/rsgis/rsnote/cp4/cp4-2.htm
9. Microwave Remote Sensing, Synthetic Aperture Radar (SAR). Available at: https://crisp.nus.edu.sg/~research/tutorial/mw.htm
10. What is Synthetic Aperture Radar (SAR)?, Sandia National Laboratories. Available at: http://www.sandia.gov/radar/what_is_sar/
11. Synthetic Aperture Radar. Available at: http://wtlab.iis.u-tokyo.ac.jp/~wataru/lecture/rsgis/rsnote/cp4/cp4-3.htm
12. Cheney, Margaret (2009) Problems in synthetic-aperture radar imaging. Inverse Problems 25. Available at: http://hdl.handle.net/10945/43818
13. Ranga Rao MS, Mahaptra PR (1997) Synthetic aperture radar: a focus on current problems. Def Sci J 47(4):517–536
14. Creating a SAR Image. Available at: http://www.pbs.org/wgbh/nova/spiesfly/rada_creating.html
15. Choo AL, Chan YK, Koo VC (2012) Geometric Correction on SAR Imagery. Progress In Electromagnetics Research Symposium Proceedings, KL, Malaysia, March 27–30
16. Toutin T (2004) Review article: geometric processing of remote sensing images: models, algorithms and methods. Int J Remote Sens 25(10):1893–1924
17. Cheney, Margaret. Introduction to Synthetic Aperture Radar (SAR) and SAR Interferometry. JPL. Available at: http://southport.jpl.nasa.gov/scienceapps/dixon/report2.html
18. Sarti F. Remote sensing and SAR images processing, characterization and speckle filtering in radar images. Available: https://earth.esa.int/c/document_library/get_file?folderId=226458&name=DLFE-2125.pdf
19. Birgir BS,Johannes RS, Benediktsson JA (2004) Combined wavelet and curvelet denoising of SAR images. In: Proceedings of IEEE 2004
20. Bhattacharya A. Speckle Filtering/Speckle Statistics, (Slide courtesy Prof. E. Pottier and Prof. L. Ferro-Famil)
21. Anil KJ (1989) Fundamentals of digital image processing, 1st edn. Prentice Hall, Inc, New Jersey
22. Chen G, Liu X (2005) Wavelet-based despeckling SAR images using neighbouring wavelet coefficients. In: Proceedings of IEEE 2005
23. Sathit Intajag and Sakreya Chitwong. (2006) Speckle noise estimation with generalized gamma distribution. SICE-ICASE International Joint Conference 2006 Oct. 18–2 1, 2006 in Bexco, Busan, Korea
24. Oliver C, Quegan S (1998) Understanding synthetic aperture radar images. Artech House, Boston
25. Bianchi T, Argenti F, Alparone L (2008) Segmentation-based map despeckling of SAR images in the undecimated wavelet domain. IEEE Trans Geosci Remote Sens 46(9):2728–2742
26. Dainty JC (1976) The statistics of speckle patterns. E. Wolf, Progress in Optics XIV © North-Holland
27. Ulaby FT, Moore RK, Fung AK (1986) Microwave remote sensing, Active and Passive, Volume III. from Theory to Applications, Artech House
28. Walessa M, Datcu M (2000) Model-based despeckling and information extraction from SAR Images. IEEE Trans Geosci Remote Sens 38(5):2258–2269

29. Escamilla HM, Méndez ER (1991) Speckle statistics from gamma-distributed random-phase screens. J Opt Soc Am A 8:1929–1935

30. Sathit Intajag and Sakreya Chitwong, (2006) Speckle Noise Estimation with Generalized Gamma Distribution. SICE-ICASE International Joint Conference, Oct 2006, 18–21, in Bexco, Busan, Korea

31. Lee J-S (1981) Refined filtering of image noise using local statistics. Comput Graph Image Process 15(2):380–389

32. Frost VS et al (1982) A model for radar images and its application to adaptive digital filtering of multiplicative noise. IEEE Trans Pattern Anal Mach Intell PAMI-4:157–166

33. Kuan DT, Sawchuk AA, Strand TC, Chavel P (1985) Adaptive noise smoothing filter for images with signal dependent noise. IEEE Trans Pattern Anal Mach Intell PAMI-7(2):165–77

34. Lopès A, Touzi R, Nezry E (1990) Adaptive speckle filters and scene heterogeneity. IEEE Trans Geosci Remote Sens 28(6):992–1000

35. Lopès A, Nezry E, Touzi R, Laur H (1990) Maximum a posteriori speckle filtering and first-order texture models in SAR images. In Proc. IEEE Int Geoscience and Remote Sensing Symp. 2409–2412

36. Lopès A, Nezry E, Touzi R, Laur H (1993) Structure detection and statistical adaptive speckle filtering in SAR images. Int J Remote Sens 14(9):1735–1758

37. Donoho DL, Johnstone IM (1994) Adapting to unknown smoothness via wavelet shrinkage. J Am Stat Assoc 90:1200–1224

38. Meer P, Park R-H, Cho K (1994) Multiresolution adaptive image smoothing. Graph Models Image Process 56(2):140–148

39. Guo H, Odegard JE, Lang M, Gopinath RA, Selesnick IW, Burrus CS (1994) Wavelet based speckle reduction with application to SAR based ATD/R. Proc IEEE Int Conf Image Process 1:75–79

40. Donoho DL (1995) Denoising by soft-thresholding. IEEE Trans Inf Theory 41(3):613–627

41. Gagnon L, Jouan A (1997) Speckle filtering of SAR images: a comparative study between a complex-wavelet-based and standard filter. Proc SPIE 80–91

42. Aiazzi B, Alparone L, Baronti S, Borri G (1998) Pyramid-based multiresolution adaptive filters for additive and multiplicative image noise. IEEE Trans Circuits Syst II 45(8):1092–1097

43. Aiazzi B, Alparone L, Baronti S (1998) Multiresolution local-statistics speckle filtering based on a ratio Laplacian pyramid. IEEE Trans Geosci Remote Sens 36(5):1466–1476

44. E. Hervet, R. Fjørtoft, P. Marthon, and A. Lopès (1998) Comparison of wavelet-based and statistical speckle filters. In: Proc. SPIE SAR image analysis, modelling, and techniques III, F. Posa, Ed. 3497: 43–54

45. Sveinsson JR, Benediktsson JA (2003) Almost translation invariant wavelet transformations for speckle reduction of SAR images. IEEE Trans Geosci Remote Sens 41(510):2404–2408

46. Solbø S, Eltoft T (2004) Homomorphic wavelet-based statistical despeckling of SAR images. IEEE Trans Geosci Remote Sens 42(4):711–721

47. Dai M, Peng C, Chan AK, Loguinov D (2004) Bayesian wavelet shrinkage with edge detection for SAR image de-speckling. IEEE Trans Geo Sci Remote Sens 42(8):1642–1648

48. Bhuiyan MIH, Ahmad MO, Swamy MNS (2005) A new homomorphic Bayesian wavelet-based MMAE filter for despeckling SAR images. In: Proc. IEEE Int. Symp. Circuits and Systems (ISCAS) 5: 4935–4938

49. Bhuiyan MIH, Ahmad MO, Swamy MNS (2007) Spatially adaptive wavelet-based method using the Cauchy prior for denoising the SAR images. IEEE Trans Circuits Syst Video Technol 17(4):500–507

50. Wu J, Yan W, Bian H, Ni W (2010) A despeckling algorithm combining curvelet and wavelet transforms of high resolution SAR images. Proc Comput Des Appl 1:302–305

51. Ranjani JJ, Thiruvengadam SJ (2010) Dual tree complex wavelet transform based despeckling using interscale dependency. IEEE Trans Geosci Remote Sens 48(6):2723–2731

52. Vijaykumar VR, Mathew A, Rao B, Santhanamari (2012) Dual tree complex wavelet transform based SAR image despeckling. In: 4th International Conference on Intelligent and Advanced Systems (ICIAS2012)

53. Tao R, Wan H, Wang Y (2012) Artifact-free despeckling of SAR images using contourlet. IEEE Geosci Remote Sens Lett 9(5):980–984

54. Argenti F, Bianchi T, Lapini A, Alparone L (2012) Fast MAP despeckling based on Laplacian–Gaussian modeling of wavelet coefficients. IEEE Geosci Remote Sens Lett 9(1):13–17

55. Chen H, Zhang Y, Wang H, Ding C (2012) Stationary-wavelet based despeckling of SAR images using two-sided generalized gamma models. IEEE Geosci Remote Sens Lett 9(6):1061–1065

56. Perona P, Malik J (1990) Scale space and edge detection using anisotropic diffusion. IEEE Trans Image Process 12(8):629–639

57. Yu Y, Acton ST (2002) Speckle reducing anisotropic diffusion. IEEE Trans Image Process 11(11):1260–1270

58. Yu Y, Acton ST (2004) Automated delineation of coastline from polarimetric SAR imagery. Int J Remote Sens 25(17):3423–3438

59. Tomasi C, Manduchi R (1998) Bilateral filtering for gray and color images. In: Proc. 6th Int. Conf. Computer Vision (ICCV) pp. 839–846

60. Zhang WG, Zhang Q, Yang CS (2011) Improved bilateral filtering for SAR image despeckling. Electron Lett 47(4):286–288

61. Li G-T, Wang C-L, Huang P-P, Yu W-D (2013) SAR image despeckling using a space-domain filter with alterable window. IEEE Geosci Remote Sens Lett 10(2):263267

62. Mastriani M, Giraldez AE (2016) Neural shrinkage for wavelet-based SAR despeckling. arXiv preprint arXiv:1608.00279

63. Buades A, Coll B, Morel J-M (2005) A non-local algorithm for image denoising. Computer Vision and Pattern Recognition CVPR 2005. IEEE Computer Society Conference on, 20–25 June 2005

64. Achim A, Kuruoglu EE, Zerubia J (2006) SAR image filtering based on the heavy-tailed Rayleigh model. IEEE Trans Image Process 15(9):2686–2693

65. Donoho DL (2006) Compressed sensing. IEEE Trans Inform Theory 52(4):1289–1306

66. Foucher S (2008) SAR image filtering via learned dictionaries and sparse representations. In: Proc. IEEE Int. Geoscience and Remote Sensing Symp. (IGARSS) I: 229–232

67. Yang M, Zhang G (2012) SAR image despeckling using over-complete dictionary. Electron Lett 48(10):596–597

68. Hao Y, Feng X, Xu J (2012) Multiplicative noise removal via sparse and redundant representations over learned dictionaries and total variation. Signal Process 92(6):1536–1549

69. Lee J-S, Wen J-H, Ainsworth TL, Chen K-S, Chen AJ (2009) Improved sigma filter for speckle filtering of SAR imagery. IEEE Trans Geosci Remote Sens 47(1):202–213

70. Lee JS (1983) Digital image smoothing and the sigma filter. Comput Vis Graph Image Process 24(2):255–269

71. Teuber T, Lang A (2012) A new similarity measure for nonlocal filtering in the presence of multiplicative noise. Comput Stat Data Anal 56(12):3821–3842

72. Gragnaniello D, Poggi G, Verdoliva L (2012) Classification based nonlocal SAR despeckling. In: Proc. Tyrrhenian Workshop on Advances in Radar and Remote Sensing 121–125

73. Jojy C, Nair MS, Subrahmaniyam GRKS, Riji R (2013) Discontinuity adaptive non-local means with importance sampling unsented Kalman filter for despeckling SA images. IEEE Trans Sel Top Appl Earth Obs Remote Sens 6(4):1964

74. Li H-C, Hong W, Wu Y-R, Fan P-Z (2013) Bayesian wavelet shrinkage with heterogeneity-adaptive threshold for SAR image despeckling based on generalized gamma distribution. IEEE Trans Geosci Remote Sens 51(4):2388–2402. https://doi.org/10.1109/TGRS.2012.2211366

75. Sethunadh R, Thomas T (2014) Spatially adaptive despeckling of SAR image using bivariate thresholding in directionlet domain. Electron Lett 50(1):44–45. https://doi.org/10.1049/el.2013.0971

76. Zhu L, Zhao X, Gu M (2014) SAR image despeckling using improved detail-preserving anisotropic diffusion. Electron Lett 50(15):1092–1093. https://doi.org/10.1049/el.2014.0293

77. Parrilli S, Poderico M (2012) Cesario Vincenzo Angelino, Luisa Verdoliva: a nonlocal SAR image denoising algorithm based on LLMMSE wavelet shrinkage. IEEE Trans Geosci Remote Sens 50(2):606–616

78. Kervrann C, Boulanger J, Coupé P (2007) Bayesian nonlocal means filter, image redundancy and adaptive dictionaries for noise removal. In: Proc. 1st Int. Conf. on Scale Space and Variational Methods in Computer Vision (SSVM) pp. 520–532

79. Coupe P, Hellier P, Kervrann C, Barillot C (2008) Bayesian non local means-based speckle filtering. In: Proc. 5th IEEE Int. Symp. Biomedical Imaging: From Nano to Macro pp. 1291–1294

80. Zhong H, Li Y, Jiao L (2011) SAR image despeckling using Bayesian non-local means filter with sigma preselection. IEEE Geosci Remote Sens Lett 8(4):809–813

81. de la Mata-Moya D, Diaz-Soria A, Martin-de-Nicolas J, Jarabo-Amores M-P, Pelaez VM (2014) Spatially adaptive thresholding of the empirical mode decomposition for speckle reduction purposes. In:10th European Conference on Synthetic Aperture Radar; Proceedings of Date of Conference: 3–5 June 2014

82. Xu B, Cui Y, Li Z, Zuo B, Yang J, Song J (2015) Patch ordering-based sar image despeckling via transform-domain filtering. IEEE J Sel Top Appl Earth Obs Remote Sens 8(4):1682–1695. https://doi.org/10.1109/JSTARS.2014.2375359

83. Zhao Y, Liu J, Zhang B, Hong W, Yirong Wu (2015) Adaptive total variation regularization based SAR image despeckling and despeckling evaluation index. IEEE Trans Geosci Remote Sens 53(5):2765–2774

84. Rudin LI, Osher S, Fatemi E (1992) Nonlinear total variation based noise removal algorithms. Physica D 60(1–4):259–268

85. Shi J, Osher S (2008) A nonlinear inverse scale space method for a convex multiplicative noise model. SIAM J Imaging Sci 1(3):294–321

86. Denis L, Tupin F, Darbon J, Sigelle M (2009) SAR image regularization with fast approximate discrete minimization. IEEE Trans Image Process 18(7):1588–1600

87. Palsson F, Sveinsson JR, Ulfarsson MO, Benediktsson JA (2012) SAR image denoising using total variation based regularization with SURE-based optimization of the regularization parameter. In: Proc. IEEE Int. Geoscience and Remote Sensing Symp (IGARSS) pp. 2160–2163

88. Gleich D, Kseneman M (2012) A comparison of regularization based methods for despeckling of SLC SAR images. In: Proc. 9th European Conf. Synthetic Aperture Radar (EUSAR) pp. 784–787

89. Atto AM, Trouvé E, Nicolas J-M, Lê TT (2016) Wavelet operators and multiplicative observation models—Application to sar image time-series analysis. IEEE Trans Geosci Remote Sens 54(11):6606–6624

90. Gragnaniello D, Poggi G, Scarpa G, Verdoliva L (2016) SAR Image Despeckling by Soft Classification. IEEE J Sel Top Appl Earth Obs Remote Sens 9(6):2118–2130

91. Sivaranjani RS, Roomi MM, Senthilarasi M (2019) Speckle noise removal in SAR images using Multi-Objective PSO (MOPSO) algorithm. Appl Soft Comput 76:671–681

92. Xu Z, Shi Q, Chen Y, Feng W, Shao Y, Sun L, Huang X (2018) Non-stationary speckle reduction in high resolution SAR images. Digit Signal Process 73:72–82

93. Rana VK, Suryanarayana TMV (2019) Evaluation of SAR speckle filter technique for inundation mapping. Remote Sens Appl Soc Environ 16:100271

94. Gokul J, Nair MS, Rajan J (2017) Guided SAR image despeckling with probabilistic non local weights. Comput Geosci 109:16–24

95. Sujitha AG, Vasuki P, Deepan AA (2019) Hybrid Laplacian Gaussian Based Speckle Removal in SAR Image Processing. J Med Syst 43(7):222

96. Liu S, Guoqing Wu, Zhang X, Zhang K, Wang P, Li Y (2017) SAR despeckling via classification-based nonlocal and local sparse representation. Neurocomputing 219:174–185

97. Lu Y, Gao Q, Sun D, Xia Yi, Zhang D (2016) SAR speckle reduction using Laplace mixture model and spatial mutual information in the directionlet domain. Neurocomputing 173:633–644

98. Farhadiani R, Homayouni S, Safari A (2019) Hybrid SAR speckle reduction using complex wavelet shrinkage and non-local PCA-based filtering. IEEE J Sel Top Appl Earth Obs Remote Sens 12(5):1489–1496

99. Ravani K, Saboo S, Bhatt JS (2019) A practical approach for SAR image despeckling using deep learning. In: IEEE International Geoscience and Remote Sensing Symposium pp. 2957–2960

100. Gu F, Zhang H, Wang C, Zhang B (2017) Residual encoder-decoder network introduced for multisource SAR image despeckling. In: 2017 SAR in Big Data Era: models, methods and applications (BIGSARDATA), pp. 1–5. IEEE, 2017

101. Denis L, Deledalle C-A, Tupin F (2019) From patches to deep learning: combining self-similarity and neural networks for SAR image despeckling. In: IGARSS 2019–2019 IEEE International Geoscience and Remote Sensing Symposium, pp. 5113–5116

102. Vitale S, Ferraioli G, Pascazio V (2019) A new ratio image based CNN algorithm for SAR despeckling. In: IGARSS 2019–2019 IEEE international geoscience and remote sensing symposium, pp. 9494–9497

103. Gleich D, Šipoš D (2019) Deep despeckling of SAR images. In: IGARSS 2019–2019 IEEE international geoscience and remote sensing symposium, pp. 1907–1910

104. Cozzolino D, Verdoliva L, Scarpa G, Poggi G (2019) Nonlocal SAR image despeckling by convolutional neural networks. In: IGARSS 2019–2019 IEEE international geoscience and remote sensing symposium, pp. 5117–5120

105. Ferraioli G, Pascazio V, Vitale S (2019) A novel cost function for despeckling using convolutional neural networks. In: 2019 Joint Urban Remote Sensing Event (JURSE), pp. 1–4

106. Gu F, Zhang H, Wang C (2020) A two-component deep learning network for SAR image denoising. IEEE Access 8:17792–17803

107. Wang P, Zhang He, Patel VM (2017) SAR image despeckling using a convolutional neural network. IEEE Signal Process Lett 24(12):1763–1767

108. Kwak Y, Song W-J, Kim S-E (2018) Speckle-noise-invariant convolutional neural network for SAR target recognition. IEEE Geosci Remote Sens Lett 16(4):549–553

109. Yue D-X, Feng Xu, Jin Y-Q (2018) SAR despeckling neural network with logarithmic convolutional product model. Int J Remote Sens 39(21):7483–7505

110. Argenti F, Lapini A, Bianchi T, Alparone L (2013) A tutorial on speckle reduction in synthetic aperture radar images. IEEE Geosci Remote Sens Mag 1(3):6–35

111. Singh P, Shree R (2017) A new homomorphic and method noise thresholding based despeckling of SAR image using anisotropic diffusion. J King Saud Univ Comput Inf Sci. https://doi.org/10.1016/j.jksuci.2017.06.006

112. Xie H, Pierce LE, Ulaby FT (2002) Statistical properties of logarithmically transformed speckle. IEEE Trans Geosci Remote Sens 40(3):721–727

113. Singh P, Shree R (2017) A new computationally improved homomorphic despeckling technique of SAR images. Int J Advan Res Comp Sci 8(3)

114. Li GT, Wang CL, Huang PP, Yu WD (2013) SAR image despeckling using a space-domain filter with alterable window. IEEE Geosci Remote Sens Lett 10(2):263267

115. Zhang L, Zhang L, Mou X, Zhang D (2011) FSIM: a feature similarity index for image quality assessment. IEEE Trans Image Process 20(8):2378–2386

116. Singh P, Shree R (2016) Speckle noise: modelling and implementation. Int J Control Theory Appl 9(17):8717–8727

117. Sattar F, Floreby L, Salomonsson G, Lovstrom B (1997) Image enhancement based on a nonlinear multiscale method. IEEE Trans Image Process 6(6):888–895

118. Achim A, Tsakalides P, Bezerianos A (2003) SAR image denoising via Bayesian wavelet shrinkage based on heavy-tailed modelling. IEEE Trans Geosci Remote Sens 41(8):1773–1784

119. Singh P, Shree R (2016) Statistical modelling of log transformed speckled image. Int J Comput Sci Inf Secur 14(8):426–431

120. Singh P, Shree R (2017) Statistical quality analysis of wavelet based sar images in despeckling process. Asian J Electr Sci 6(2):1–18

121. Singh P, Shree R (2017) Quantitative dual nature analysis of mean square error in SAR image despeckling. Int J Comput Sci Eng 9:619–622

122. Singh P, Shree R (2016) Analysis and Effects of Speckle Noise in SAR Images. In: 2nd International conference on advances in computing, communication, and automation (ICACCA) 1–5. (IEEE International Conference)

123. Benitz GR (1997) High-definition vector imaging. Lincoln Lab J 10(2):147–170

124. M Çetin, WC Karl, and DA Castañon (2000) Evaluation of a regularized SAR imaging technique based on recognitionoriented features. In: Proceeding SPIE algorithms for synthetic aperture radar imagery VII 4053: 40–51

125. Mastriani M, Giraldez AE (2016) Enhanced directional smoothing algorithm for edge-preserving smoothing of synthetic-aperture radar images. arXiv preprint arXiv:1608.01993

126. Synthetic Aperture Radar (SAR) Imagery, Sandia National Laboratories, Airborne ISR. Available at: http://www.sandia.gov/RADAR/imagery/

127. Moreira A, Prats-Iraola P, Younis M, Krieger G, Hajnsek I, Papathanassiou KP (2013) A tutorial on synthetic aperture radar. IEEE Geosci Remote Sens Mag. https://doi.org/10.1109/MGRS.2013.2248301